DESCRIPTION OF COHERENT PROPERTIES OF A COPPER–VAPOR LASER EMISSION

V.V. Kolosov and V.O. Troitskii

Institute of Atmospheric Optics,
Siberian Branch of the Russian Academy of Sciences, Tomsk
Received April 27, 1993

It is proposed to assume that in many practical cases an actual light beam can be presented as a combination of components that differ in power and divergence. Not very complicated series of theoretical and experimental investigations enabling one to determine radii of coherence and power of these components is proposed. It is shown that a three-component theoretical model, constructed according to this technique quite well describes propagation of the radiation of the Cu*-vapor laser under study in the far zone of propagation.*

1. INTRODUCTION

Hundreds of original papers, overviews, and monographs devoted to studies of properties of copper–vapor laser (CVL) emission can be found in literature. Quite vast bibliography can be found, for example, in Ref. 1. It should be noted that among the parameters determining behavior of the CVL, the beam power and divergence are most important for many practical applications of lasers. Therefore in this paper we shall consider just these characteristics or, in other words, the spatial and energy structure (SES) of CVL radiation.

By omitting a discussion of physical processes of the output CVL beam formation we would like to note only the most important, from our point of view, circumstances.[2,3] First, the use of an unstable resonator (UR) provides maximum power at minimum divergence. Second, the CVL radiation generated in a UR is composed of several components (modes[4]) each being characterized by its own values of the mean power and divergence. And finally, these properties strongly depend on the laser construction, the type of UR, and on operating conditions of a CVL.

In this connection, it seems to be obvious, that some simple researches are advisable prior to using a CVL that could provide obtaining information about the number of emission components of a CVL, their power and divergence. One of possible ways of acquiring such an information is considered in this paper. Results of this study are summarized in a mathematical model of the output CVL beam, the validity of which is checked by comparing with the experimental data.

2. EXPERIMENTAL SETUP AND TECHNIQUE

In our experiments we used a CVL active element "Kulon" with a 30 cm long and 1.2 cm in diameter active zone. The laser delivered pulsed radiation at a pulse repetition frequency of 6 kHz. Total mean power of radiation at both green and yellow lines was 1.3 W (0.8 W at the wavelength 510.6 nm which was used in the experiments).

Optical arrangement of the experimental setup is shown in Fig. 1. The active element *1* was placed inside a confocal unstable resonator, arranged between two totally reflecting spherical mirrors with the focal lengths of 100 and 6 cm, respectively. The escape of radiation from the cavity was performed with a plane–parallel mirror *4*. The coupling diaphragm with the diameter 0.8 mm was placed at the point of common focus of the mirrors *2* and *3*.

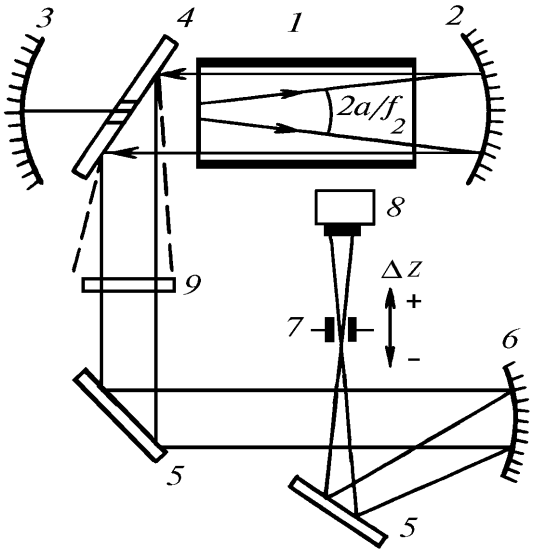

FIG. 1. Block diagram of the experimental setup.

Information about SES of a CVL beam has been extracted from two characteristics measured experimentally. The first one is the transmission of the coupling diaphragm *7* placed at the caustic of a spherical mirror *6*

$$\eta = \eta(\omega) = P_{\omega} / P ,$$

where P and P_x are the mean power of radiation, incident onto the diaphragm and passed through it. Measurements were carried out for 10 values of the diaphragm radius from $\omega_{min} = 125$ to $\omega_{max} = 920$ μm. Second, the function $\eta = \eta(\Delta z)$ was studied, where Δz is the distance between the diaphragm *7* ($\omega = 700$ μm) and the caustic (see the arrow in Fig. 1). The value of Δz varied in the range from – 30 to + 30 cm.

Experiments were carried out with two spherical mirrors *6*. Focal lengths of the mirrors were 155 and 207 cm. An UMO–2 power meter *8* and an interference

0235-6880/93/08 580-05 $02.00

filter were used for measuring the emission power and isolating the green line of the CVL emission.

3. THEORETICAL MODEL

First of all, it is necessary to solve the problem on the number of components in the output beam of the CVL with UR.

Let us assume, that the formation of laser radiation in an UR is as follows. Spontaneous emission, propagating along the direction towards the coupling hole escapes from the cavity in the form of a widely diverging superradiance (see the dashed line in Fig. 1). Spontaneous emission reflected from mirror *2* and passed again through the amplification zone forms, as it is called, a single–pass generation. The portion of this emission confined by the cone of angular aperture $2a/f_2$, where a is the radius of the active zone, escapes from the resonator in the form of almost parallel beam. In fact, just this portion of laser emission makes the main contribution to the formation of the output laser beam when successively travelling through the UR. Since in our case of 20–ns pulse duration only three round trips of the emission can occur inside the cavity, we shall consider a three–component model which takes into account the single pass emission as the background, the beam formed due to double round trips as an intermediate radiation, and the core formed after three round trips of the emission inside the UR. (According to terminology from Ref. 3). Comparatively low power superradiance is neglected in this model.

Since in the case under study we deal with a partially coherent light, we shall make use, as it is usual,[5] a transverse function of coherence for describing its propagation. We assume that the initial distribution of a coherence function for each of the three components is as follows:

$$\Gamma_i(\alpha, \beta, z=0) = I_{0i} \exp\left\{-\frac{2\alpha^2}{a_i^2} - \frac{\beta^2}{2l_i^2} + i\,\kappa\frac{\alpha\beta}{R_i}\right\},\ i = 1, 2, 3, \quad (1)$$

where $\alpha = (\mathbf{r}_1 + \mathbf{r}_2)/2$, $\beta = \mathbf{r}_1 - \mathbf{r}_2$, a_i determines the distribution of the mean intensity, R_i is the radius of a curvature of the average wavefront; $l_i = a_i L_i/\sqrt{L_i^2 + 2a_i^2}$, L_i is the radius of coherence, z is the axis along the beam ($z = 0$ is the position of the mirror *6* in Fig. 1), and $\mathbf{r}$ is the radius–vector in the plane perpendicular to the propagation axis.

Two approximations were used in Eq. (1): that is the dependence of Γ_i on the difference (β) and sum (α) coordinates was assumed to be Gaussian. The first assumption is rather common and it is valid under sufficiently general restrictions imposed on the amplitude and phase fluctuations of the radiation.[5] The second assumption is, strictly speaking, arbitrary and we use it only to alleviate analytical calculations. However, it is known,[5] that the intensity distribution in the far zone and, consequently, in the focal plane (which we are interested in) is determined by the initial distribution of the coherence function over the difference coordinate and does not depend on the initial intensity distribution. The boundary conditions in the form of Eq. (1) can be considered quite acceptable for description of the intensity distribution in the vicinity of geometrical focus of a lens.

Using Eq. (1) one can easily show[5] that in the vicinity of geometrical focus of a lens with the focal length f the average intensity of each component is determined by the expression

$$I_i(r) \sim P\,Q_i \exp(-2r^2/\rho_i^2), \quad (2)$$

where P is the total mean power of the beam, Q_i is the contribution coming from each component to the total power

$$\rho_i = \sqrt{z^2 a_i^2 (1/z - 1/f_i')^2 + 4z^2/\kappa^2 l_i^2}, \quad (3)$$

where $f_i' = f R_i/(R_i - f)$, $\kappa = 2\pi/\lambda$, and z is the distance from the lens. In the plane of geometrical focus we have

$$z = f' \ \text{ and } \ \rho_i = 2z/\kappa l_i. \quad (4)$$

4. DATA PROCESSING

As follows from the above discussion the beam intensity in a plane at a distance z from a lens is

$$I = \sum_{i=1}^{3} I_i = \sum_{i=1}^{3} I_{0i} \exp(-2r^2/\rho_i^2) =$$
$$= (2P/\pi) \sum_{i=1}^{3} (Q_i/\rho_i^2) \exp(-2r^2/\rho_i^2).$$

The power P_ω, passed through the hole with radius ω is determined by the integral:

$$P_\omega = 2\pi \sum_{i=1}^{3} \int_0^\omega I_i(r)\, r\, dr = P \sum_{i=1}^{3} Q_i [1 - \exp(-2\omega^2/\rho_i^2)] =$$
$$= P \sum_{i=1}^{3} Q_i W_i.$$

Then for the transmission coefficient η we have

$$\eta = \eta(\omega) = \sum_{i=1}^{3} Q_i W_i. \quad (5)$$

Let the transmission coefficients for two diaphragms with radius $\omega = \omega_j$, $j = 1, 2$ be known. In this case we have three equations

$$\sum_{i=1}^{3} Q_i W_{ij} = \eta_j, \ j = 1, 2; \ \sum_{i=1}^{3} Q_i = 1, \quad (6)$$

where

$$W_{ij} = 1 - \exp(-2\omega_j^2/\rho_i^2).$$

If all W_{ij} are known, the system of Eqs. (6) transfers into the system of equations for three unknown coefficients Q_i. The solution of system (6) is

$$Q_1 = D_1/D, \ Q_2 = D_2/D, \ Q_3 = 1 - D_1/D - D_2/D, \quad (7)$$

where

$$D = (W_{11} - W_{31})(W_{22} - W_{32}) - (W_{21} - W_{31})(W_{12} - W_{32}),$$
$$D_1 = (\eta_1 - W_{31})(W_{22} - W_{32}) - (\eta_2 - W_{32})(W_{21} - W_{31}),$$
$$D_2 = (\eta_2 - W_{32})(W_{11} - W_{31}) - (\eta_1 - W_{31})(W_{12} - W_{32}).$$

Here we would like to note one circumstance. If the condition $\omega_j \gg \rho_j$, $j = 1, 2$ is fulfilled, then

$$D \to (1 - W_{31})(1 - W_{32}) - (1 - W_{31})(1 - W_{32}) = 0 ,$$

and the solution of Eq. (7) becomes senseless. Figure 2 shows the response of the solution of Eq. (7) to the errors in experimental measurements of $\eta = \eta(\omega)$. It presents the rms error σ_i as a function of relative error ε_i of η_i measurements. Assume also that only four first values of η_i corresponding to four smallest diaphragms of a series of ten diaghragms used in the experiment are measured with an error. Thus,

$$\tilde{\eta}_j = \eta_j (1 + \varepsilon_j) , \quad j = 1, 4 ,$$

where Gaussian random value ε_i has the zero average value and variance σ_e^2.

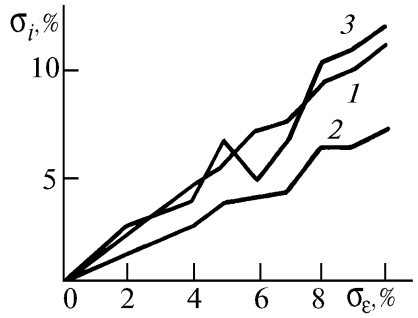

FIG. 2. The dependence of rms error σ_i in determining fraction coefficients for power of core (1), intermediate (2), and background (3) beams on the error σ_ε in $\eta = \eta(\omega_j)$ measurements for four the least ω_j values.

The results of numerical simulations are summarized by the expression

$$\sigma_j = \sqrt{\frac{1}{N}\sum_{i=1}^{N} (\tilde{Q}_{in} - Q_i)^2} \Big/ Q_i ,$$

where Q_i are the exact values of the fraction coefficients and $\tilde{Q}_{in}$ are those, obtained in each of $N = 400$ simulation cycles.

5. SEQUENCE OF OPERATIONS

First of all we experimentally find the function $\eta = \eta(\Delta z)$ and determine the value z_f where $\eta(z_f) = \eta_{max}$. Then we measure the function $\eta = \eta(\omega)$ in the plane $z = z_f$. Further processing assumes several stages.

At the first stage we suppose all R_i to be of the same value that means that all three components have their caustics at the plane $z = z_f$. As a result,

$$f_i' = z_f = R_i f / (R_i - f) , \quad i = 1, 2, 3 ,$$

and, in addition, expression (4) holds true for all ρ_i.

Then we take arbitrarily two experimental values of $\eta_j = \eta(\omega_j)$, $j = 1, 2$. Also arbitrarily (but so that $l_1 > l_2 > l_3$) we take three values for l_i. Here and below we designate the characteristics of the core, intermediate, and background radiation by indices 1, 2 and 3, respectively. Substitute these l_i values in Eq. (4) and calculate three values of ρ_i. Then the values η_j, ω_j, and ρ_i are substituted in Eq. (7) and we find Q_i values.

Two sets of three parameters Q_i and l_i obtained in this way describe the behavior of the curve $\eta = \eta(\omega)$, so that it coincides with two preselected experimental points. By varying the values l_i one can achieve the best fitting between the theoretical and experimental curves.

Taking another pair of experimental values we then go through the same procedure again. Finally, by averaging (over the number of pairs used) we obtain mean values $\overline{Q}_i$ and $\overline{l}_i$, which are considered as the final results.

Now it is necessary to construct theoretical function $\eta = \eta(\Delta z)$ using Eq. (3) and thus obtained values $\overline{Q}_i$ and $\overline{l}_i$ and to match it to the experimental one by varying the quantities a_i from Eq. (3). It can happen so that for the best fitting of the plots we are forced to ignore the assumption on equality of R_i values. In this case we should do the following. Since the above–obtained value z_f strongly depends on the distance between the mirrors *2* and *3* of the UR (see Fig. 1), we can align the UR so that $z_f = f$, where f is the focal length of the mirror *6*. In this case it can be assumed quite correctly that

$$R_1 = \infty > R_2 > R_3 .$$

Thus, to achieve the best fitting between the theoretical function $\eta = \eta(\Delta z)$ and the experimental one it is necessary to find proper values of the five sets of parameters: a_i, R_2, and R_3.

At the second stage it is necessary to correct the values $\overline{Q}_i$ and $\overline{l}_i$ using already at the first step formula (3) instead of Eq. (4) and a_i and R_i found. Using thus corrected $\overline{Q}_i$ and $\overline{l}_i$ values we have to find a_i and R_i again and so on. Reiterations are being done until the changes of the sought values become negligible. Estimates show that already at the second stage the values, for example, $\overline{Q}_i$ differ from the initial ones by less than 0.5%, that is, in many cases one iteration is quite sufficient.

6. MEASUREMENT RESULTS AND CONCLUSIONS

Following the above procedure we have carried out measurements using two mirrors *6* with the focal lengths $f = 155$ and 207 cm. The values $\overline{Q}_i$ and $\overline{l}_i$ obtained in this way are shown in Table I.

TABLE I.

Parameters	z_f, cm		
	155	207	Averaged over two z_f
$\overline{l}_1, \overline{l}_2, \overline{l}_3$,cm	0.25, 0.058, 0.01	0.25, 0.056, 0.008	0.25, 0.057, 0.009
$\overline{Q}_1, \overline{Q}_2, \overline{Q}_3$,%	22.8, 57.9, 19.3	22.5, 62.4, 15.1	22.65, 60.15, 17.2

Figure 3 shows experimental (dots) and theoretical (solid line) functions $\eta = \eta(\omega)$. Averaged (over z_f) values of $\overline{Q}_i$ and $\overline{l}_i$ (the third column in the table) were used for calculations.

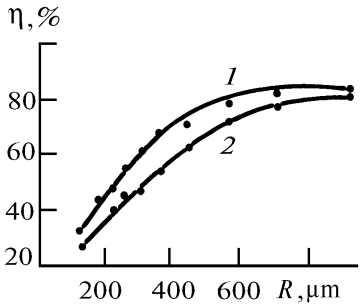

FIG. 3. Transmission coefficient for the diaphragm placed in the focal plane of a mirror, as a function of the diaphragm radius. 1) the focal length of the mirror f = 155 *and 2)* f = 207 cm.

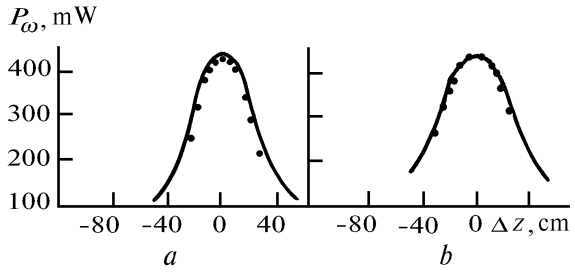

FIG. 4. The power of radiation passed through the diaphragm with the radius ω = 700 μm, *as a function of the distance between the diaphragm and the focal plane of the mirror with* f = 155 cm *(a) and* f = 207 cm *(b).*

Theoretical functions $P_\omega = P_\omega$ (Δz, ω = 700 μm) were calculated using these values of $\overline{Q}_i$ and $\overline{l}_i$ as well as assuming that $a_1 = a_2 = 0.56$ cm, $a_3 = 1.8$ cm, $R_2 = 18 \cdot 10^3$ cm, and $R_3 = 10^3$ cm. Results are presented in Fig. 4. Corresponding experimental values are shown by dots.

Rather good agreement of the theory and experiment allows us to assume that expression (1) is a suitable model of a CVL beam formed in UR as far as it concerns the intensity distribution in the far zone (points corresponding to the maximum Δz in Fig. 4 drop out).

In principle, the proposed procedure is rather simple and convenient. Really, a researcher has only to measure the functions $\eta = \eta(\omega)$ and $\eta = \eta(\Delta z)$ and use them in calculations. The number of experimental points can be reduced to 3 or 4 and the main problem is to measure these values as accurate as possible. Two circumstances help to solve this problem. First, the function $\eta = \eta(\omega)$ should be smooth and monotonic. Second, the measured η value can be only smaller or equal to the actual one. This allows one to correct the results during measurements.

Let us note basic drawbacks, from our point of view, of the proposed procedure. Unfortunately, all parameters of the background except for Q_3, are determined very arbitrarily, that is the behavior of plots in Figs. 3 and 4 only weakly depends on them. Then, the necessity of fitting some parameters should be mentioned. Of course, we would like to complete the system of equations (6) by three equations and to solve the system of six equations for six unknown $\overline{Q}_i$ and $\overline{l}_i$ variables. However, this possibility seems to be too problematic now.

CONCLUSION

Thus, it can be noted that the use of three component model is well justifiable only for the particular object of our study. If necessary, the developed procedure can be easily extended to the case of an arbitrary number of output radiation components. We think also that this technique can be applied without principal changes to any laser and nonlaser radiation with Gaussian statistics under one condition that the degree of radiation monochromaticity is so high that chromatic aberrations can be neglected.

REFERENCES

1. A.N. Soldatov and V.I. Solomonov, *Gas–Discharge Lasers on Self–Restructed Transitions in Metal Vapors* (Nauka, Novosibirsk, 1985), 150 pp.
2. A.A. Isaev and G.G. Petrash, Tr. Phys. Inst. Akad. Nauk SSSR **206**, 116 (1991).
3. V.V. Zubov, N.A. Lyabin, and A.D. Chursin, Kvant. Elektron. **13**, No. 12, 2431 (1986).
4. Yu. A. Anan'ev, Kvant. Elektron. **2**, No. 6, 1138 (1975).
5. S.M. Rytov, Yu.A. Kravtsov, and V.I. Tatarskii, *Introduction into Statistical Radiophysics. Part 2. Random Fields* (Nauka, Moscow, 1978), 468 pp.